To be presented at the Hokkaido University Symposium on Effective Utilization of Surface Analysis Techniques in Plasma Surface Interactions, October 4-7, 1982, Hokkaido University, Sapporo, Japan

CONF-821045--3

SPUTTER-INDUCED EROSION OF ALKALI METAL SURFACES - AES, XPS and SIMS STUDIES*

CONF-821045--3

DE83 007720

Alan R. Krauss

Chemistry Division, Argonne National Laboratory, Argonne, IL 60439

Abstract

This paper will discuss the manner in which the techniques of Auger-electron spectroscopy (AES), X-ray-photoelectron spectroscopy (XPS), secondary-ion mass spectroscopy (SIMS), and ion-scattering spectroscopy (ISS) may be used to study the use of high secondary-ion-yield surfaces as a means of reducing plasma-impurity influx in magnetic-confinement fusion devices.

DISCLAIMER

This report was prepared as an account of work sponsored by an agency of the United States Government. Neither the United States Government nor any agency thereof, nor any of their employees, makes any warranty, express or implied, or assumes any legal liability or responsibility for the accuracy, completeness, or usefulness of any information, apparatus, product, or process disclosed, or represents that its use would not infringe privately owned rights. Reference herein to any specific commercial product, process, or service by trade name, trademark, manufacturer, or otherwise does not necessarily constitute or imply its endorsement, recommendation, or favoring by the United States Government or any agency thereof. The views and opinions of authors expressed herein do not necessarily state or reflect those of the United States Government or any agency thereof.

NOTICE

PORTIONS OF THIS REPORT ARE ILLEGIBLE. It has been reproduced from the best available copy to permit the broadest possible availability.

*Work performed under the auspices of the Office of Basic Energy Sciences, Division of Materials Sciences, U. S. Department of Energy.

MASTER

The submitted manuscript has been authored by a contractor of the U. S. Government under contract No. W-31-109-ENG-38. Accordingly, the U. S. Government retains a nonexclusive, royalty-free license to publish or reproduce the published form of this contribution, or allow others to do so, for U. S. Government purposes.

DISTRIBUTION OF THIS DOCUMENT IS UNLIMITED

EJB

INTRODUCTION

Sputter-induced erosion is one of the principal mechanisms of impurity release in magnetic-confinement fusion devices. Since the energy lost to line radiation increases very rapidly with the atomic number of the impurity atoms, it is especially important to limit the concentration of high Z atoms in the plasma. There are basically three approaches to this problem. One approach is to limit the impurity influx to the plasma by using only those high Z materials with a very low light ion sputtering yield. If however, the self-sputtering yield is greater than unity at the energy at which re-deposited impurity atoms impinge upon surfaces exposed to the plasma, there is a possibility of run-away self sputtering even if the light ion sputtering yield is very low.

A second approach is to use low Z materials for all surfaces exposed to the plasma. Because of the brittleness and poor thermal conductivity of most proposed low Z materials, it is necessary that they be used in the form of a thin coating on a structural substrate such as copper. The requirement that the coating be thin is especially critical in areas such as the limiter which are subjected to severe mechanical and thermal shock. Long term maintenance of a thin coating is rendered difficult by the fact that material is preferentially removed from the wall and deposited in a non-uniform fashion at the limiter. It is therefore desirable to provide a means of limiting the build-up of coating material at some structures while simultaneously preventing erosion at other structures or replenishing the material in-situ.

This goal is met in part by the third basic method of impurity control, namely that of controlling impurity transport. The principal device used for this purpose, the magnetic divertor, reduces self-sputtering and build-up at the limiter by removing sputtered atoms as they enter the scrape-off region. Recycling to the wall and limiter is therefore reduced, but the material removed results in a corresponding increase in net erosion.

A significant factor affecting the transport of impurities is the charge state of the sputtered atoms. In most Tokamak reactor designs, it is expected that the sheath potential will substantially exceed the kinetic energy of

the sputtered atoms. Consequently, an atom ejected from the limiter as a positive secondary ion will be returned to the surface within a few hundred microns of its point of origin. The probability that a secondary ion will *not* be immediately returned to the surface can be estimated on the basis of rather simple arguments. (1) The results are shown in Figure 1 for FED and STARFIRE design parameters. In both cases the probability is negligible. It should be noted that the sheath potential only exists in a region within a few Debye lengths of the limiter ($\sim$100 μm) and the ionization length is typically several cm. Consequently the sheath potential can not be expected to produce the immediate return of sputtered neutral atoms as a result of collision-induced ionization.

At the wall, the magnetic field is largely tangential and ejected atoms must cross magnetic field lines to reach the plasma. Secondary ions are therefore returned to the surface within approximately one gyro-radius of the point of origin. Since the gyroradius is comparable with the Debye length, the probability that a secondary ion created at either the first wall or the limiter can reach the plasma is in the range 10^{-4} to 10^{-6}.

As shown in Figure 2, (2) the secondary ion fraction for sputtering from clean metal surfaces (open symbols) is typically less than a few percent and the above-described processes are not normally expected to be significant in a plasma device. However, for some metal oxides (filled symbols) and alkali metals (x) the secondary ion fraction is in the range 50-95%. Although neither class of materials is considered to have ideal properties for use in a Tokamak environment, it appears fruitful to study the conditions leading to such high secondary ion fractions in order to determine if those conditions can be maintained in a Tokamak environment.

EXPERIMENTAL

The experimental layout is shown in Figure 3. The sample is mounted on a heatable stage in an ultra-high vacuum system containing a double-pass cylindrical mirror electron energy analyzer with coaxial electron gun, a differentially pumped ion gun, a secondary ion mass and energy analyzer and time-of-flight ion scattering spectrometer. The geometry is such that it is possible to perform three simultaneous experiments, recording the data on

three independent data channels without moving the sample. One data channel is used by the secondary ion analyzer, providing either the standard SIMS mass spectrum for secondary ions in a specified kinetic energy window, or a kinetic energy distribution for a specified m/e value. A second channel is used by the electron energy analyzer for either AES or XPS data. AES is used to provide composition information in a region within 3-10 Å of the surface. XPS is used to measure the elemental composition of a region up to ~40 Å thick and to provide information on the chemical state of each element. The third data channel corresponds to the ISS experiment which is still under development. The ISS data is complimentary to the data on the other two channels in that it can be readily calibrated to provide absolute concentrations and is sensitive to the uppermost monolayer only.

Scan control and data acquisition are controlled by an LSI-11 computer. The electron beam and ion beam positions can be adjusted manually, rastered, or placed under program control by the computer. Typically the ion and electron beams are centered on a common point and the ion beam is rastered to minimize crater edge effects. The electron beam is either rastered to minimize beam damage or placed under program control to study inhomogeneities in surface composition. In a single scan, three spectra consisting of up to 1024 points each are recorded. Seventy such scans can be stored on a single 8" diskette. Each scan may be divided into up to ten data "windows", each window encompassing a single peak or arbitrary segment of the continuous scan.

The ion source is a modified version of a commercially available differentially-pumped ion gun, with a useful energy range of 500 to 5000 eV. For hydrogen sputtering, a mass separated beam is desired. For ISS measurements with a time-of-flight spectrometer, it is necessary to pulse the ion beam very rapidly (10-40 nsec pulse width). Both of these requirements are met by installing a Wien (ExB) filter in front of the ion gun. The sputtering gas pressure is measured directly in the ionization region of the ion gun and the signal is fed back to a servo-controlled gas admission valve. The ion beam can consequently be stabilized to within a few percent for periods of time in excess of one week.

RESULTS

It is an empirical fact of secondary ion mass spectroscopy that alkali metal impurities present in amounts so small as to be totally undetectable by such techniques as Auger spectroscopy often account for the dominant secondary ion yield. In the majority of experiments to date, the alakali metal has been uncharacterized, both as to the concentration at the surface and as to such properties as bond character which might play a key role in determining the charge state of the sputtered atoms. Because the alkali metal is normally present only as a trace impurity, it is germane to ask if there is any difference between the secondary ion fraction of sputtered bulk alkali metal and that of alkali metal atoms sputtered from a matrix of less electro-positive metal.

In order to answer this question, we deposited (3) both multilayer and sub-monolayer potassium films on a molybdenum substrate, monitoring the surface potassium concentration by XPS or AES. After deposition, the ion beam was turned on and the erosion rate and secondary ion yield were simultaneously monitored by XPS or AES and SIMS.

The secondary ion fraction was determined by measuring the erosion rate of the alkali metal film both in the presence and absence of an applied electric field. Representative results for 700 eV He^+ sputtering are shown in Figure 4. For surface concentrations of potassium exceeding one monolayer as calibrated by AES, the application of an electric field had no effect on the erosion rate, indicating that almost all the potassium was sputtered as neutral atoms. For sub-monolayer coverages the erosion rate was nearly half that of the multilayer film and could be further reduced by an additional factor of 2 by applying a bias voltage to the sample. For a 45 V bias, 58% of the sputtered K atoms were returned to the surface.

Measurements of the K^+ secondary ion yield (Figure 5) showed that in the multilayer regime the K^+ yield increased as the potassium surface concentration decreased, indicating a secondary ion fraction increasing as the coverage decreased. In the monolayer regime, the secondary ion yield decreased at the same rate as the potassium concentration, indicating a constant ion fraction. The quantitative form of the data of Figure 4 was

found to be consistent with a mechanism in which K atoms in the second layer shield the first monolayer from sputtering and are eroded almost entirely as neutral atoms while the secondary ions originate almost entirely in the first monolayer, i.e. the layer in direct contact with the Mo substrate.

Although it does not entirely characterize the secondary ion formation process for alkali metals, this result indicates that the character of the nearest-neighbor bond plays a critical role in determining the charge state of the sputtered alkali metal atom. For most materials, velocity-dependent neutralization processes result in preferential neutralization of secondary ions sputtered with low kinetic energy. Consequently, the high energy tail of the secondary ion energy distribution falls more slowly than the E^{-2} behavior expected for the totality of particles sputtered by the collision cascade process (4). (Figure 6). For alkali metals, the high energy tail of the kinetic energy distribution exhibits an E^{-2} character, indicating that neutralization processes are insignificant for alkali metal secondary ions.

It is well-known that sputtering of a cesiated surface tends to result in the ejection of both Cs^+ and negative ions of the substrate material (5). In most cases the negative ion fraction is lower than the Cs positive secondary ion fraction. Consequently our present approach is to try to design a surface in which the erosion of the substrate metal is substantially reduced by the presence of an alkali metal overlayer. The alkali metal should therefore have four properties: (1) it should sputter almost entirely as secondary ions, (2) it should have low atomic number, (3) it should provide effective shielding of the substrate metal and (4) it should be possible to maintain the coating in-situ. The first and, as will be discussed below, the fourth condition favor the use of lithium, while the second and third conditions tend to favor a heavier alkali metal.

The ion fraction of alkali metal atoms evaporated from a hot metal surface is described by the Saha-Langmuir equation (6,7)

$$n^+/n \sim \exp[-(I-\phi)/kT] \qquad (1)$$

where n is the total number of atoms evaporated, n^+ the total number of ions, I is the ionization potential of the sputtered atom, ϕ is the

work function, k is Boltzmann's constant and T is the temperature. In general, lithium will evaporate from a given surface with a lower ion fraction than cesium, although it is to be noted that ion fraction values exceeding 0.9 (8) have been observed for the evaporation of lithium from some surfaces. Sputtering does not correspond to the same physical process as evaporation although the secondary ion fraction can usually be described in terms of Equation 1 if T is taken as an appropriate "effective" temperature. Empirically T is usually found to have a value of 3000-4000°K, (9) favoring a higher ion fraction by sputtering than by evaporation. Determination of the secondary ion fraction of lithium sputtered from various surfaces is proceeding in our laboratory.

Because of its low atomic number, Li is not as effective at shielding the substrate as the other alkali metals. The partial sputtering yields of Li and Cu for deuteron bombardment of a copper surface covered by one monolayer of lithium have been calculated by a modified version of the TRIM computer program, (10) with results shown in Figure 7. Depending on the deuteron kinetic energy, the Li overlayer reduces the copper erosion by 3-10x. The presence of a hydrogen layer over the lithium increases this factor to 7-200x. The lithium sputtering rate is comparable with the sputtering rate of bare copper. Because of its lower mass, the self-sputtering yield of Li is much lower than that of Cu. Consequently the plasma edge temperature corresponding to a self-sputtering yield ≥ 1 is increased. For bare copper, runaway self sputtering is calculated by TRIM to occur for an incident energy of 150 eV. The presence of a lithium overlayer raises this value to 800 eV. (11) Although lithium is not the best alkali metal with regard to all four criteria specified above, it may provide a sufficiently high secondary ion fraction and adequate shielding to make it useful as a protective overlayer.

An additional factor favoring lithium concerns the maintenance of the overlayer. Films with thickness of one monolayer can not be maintained in a Tokamak environment by periodic *ex-situ* or even *in-situ* replacement. Rather, they must be replaced on a continuous basis. Much of this replacement will occur automatically if the erosion occurs as secondary ion emission, but a means of continually replenishing lost material is clearly desirable.

Lithium forms stable alloys with a number of metals. For most of these alloys it is predicted that at t' . expected operating temperatures of a Tokamak reactor first wall and limiter, Gibbsian segregation should result in a surface lithium concentration approaching 100%, even for alloys with very low bulk lithium concentration (10,12) (Figure 8). In addition, the lithium depth profile of a dilute lithium-bearing alloy corresponds closely to that of a single Li monolayer i.e. the region of high lithium concentration does not extend beyond the first monolayer (Figure 9)

The actual lithium depth profile obtained in a fusion device will differ from that of Figure 9 because radiation-induced effects will strongly alter the depth distribution from that produced by Gibbsian segregation alone. (13) Radiation-induced segregation (RIS) may promote the enrichment of either component in a region ranging from the surface to a depth much greater than the range of the incident projectile. (14) Radiation-enhanced diffusion (RED) increases the rate at which thermal diffusion processes occur by as much as several orders of magnitude. The segregating species will be the one which would be enriched by the thermal process alone. Recoil implantation (RI) shifts surface material deeper into the bulk, and preferential sputtering (PS) will tend to deplete the surface alkali metal.

Ion scattering spectroscopy is an ideal means of measuring the surface Li concentration because it can readily be made quantitative (15) and because it is sensitive only to the uppermost monolayer although the sensitivity for Li is ∿3-10x lower than elements with z = 15-30 (16). This technique is under development in our laboratory. SIMS is nearly as surface specific, especially for light ion sputtering, but because the secondary ion fraction is one of the properties being studied, it is difficult to use the technique as a quantitative measure of surface concentration. XPS can provide roughly quantitative measures of the concentration averaged over a depth of several tens of Angstroms. The elemental sensitivity of XPS for lithium is 1/10 that of aluminum and only 0.3% that of copper. (17) Since the Lils line is within 20 eV of the Al2p and Cu3p lines, it is expected that XPS will provide poor sensitivity for Li in Al and Cu matrices. Sensitivity for the Li(KLL) Auger line is within a factor of three of the

Cu(LMM) line and only a factor of two lower than the Al(LMM) line. (18) Since all three lines correspond to Auger electrons with kinetic energies between 40 and 70 eV, it is to be expected that AES will provide good surface sensitivity for these elements, although quantitiative analysis may be hampered by partial overlap of these lines.

The lithium secondary ion signal for a typical heating sequence is shown in Figure 10 for a dilute alloy of Li in Al. (19) The Li^+ signal started to increase as soon as the sample heater was turned on, reaching equilibrium at the same time the sample attained thermal equilibrium for temperatures up to 300°C. Upon further heating (Figure 11) the Li^+ signal kept increasing long after the sample reached thermal equilibrium, eventually reaching a value 22 times greater than the initial signal. Assuming that the Li^+ secondary ion fraction is constant and that the original Li^+ signal represented the bulk concentration of 0.32%, the secondary ion signal corresponds to a surface lithium concentration of 7%. This value is in good agreement with the 7.5% value obtained by AES. Based on literature values (20) for the secondary ion fraction of bare aluminum, the observed Li^+ signal corresponds to a lithium secondary ion fraction of $\sim$20%.

Concurrently, the aluminum secondary ion yield dropped to 45% of its initial value. This result can be interpreted as the effect of physical shielding by the segregated lithium. If the segregation is limited to the uppermost monolayer TRIM predicts that a Li coverage of 0.69 is required to account for the observed decrease in Al^+. Alternatively, the decreased Al^+ secondary ion yield can be interpreted as resulting from a decreased Al^+ secondary ion fraction associated with the increased lithium concentration.

Prior to heating, no lithium signal was observed in the XPS spectrum. Upon heating, a line was observed to grow in at 64 eV, an 8 eV shift from the nominal position of 56 eV for elemental Li, corresponding to a bond that is more than 60% ionic in character. Because of the low XPS sensitivity for lithium, this signal would correspond to a lithium concentratio much greater than 7% in the 30-40 Å region sampled. The Al2s and Al2p binding energies were unshifted from the metallic values, and it is therefore important to know the depth distribution of the lithium in order to completely interpret the XPS data.

In order to obtain adequate sensitivity and depth resolution, SIMS was selected as the means of determining the lithium depth profile. The sample was heated to 490°C while monitoring the Li^+ signal. After the signal reached equilibrium, the ion beam was turned off and after a few minutes, the heater was also turned off. Once the sample was near room temperature, the ion beam was turned back on and the Li^+ signal was monitored. The results are shown in Figure 12. The signal was observed to decay rapidly from a very high level to a level slightly higher than that obtained prior to turning the ion beam off. The rate of decrease was analyzed in terms of an erosion rate for a lithium monolayer on the aluminum, and the value obtained for the sputtering yield was identical with the value predicted by TRIM for the erosion of a lithium overlayer on aluminum. The time during which this behavior was observed was equal to the time required to remove one monolayer. Subsequently a much slower rate of decrease was observed during which the Li^+ signal decreased by an order of magnitude before returning to a stable value corresponding to that obtained prior to sample heating. The material removed corresponded to a sputter-profiled depth of 3000 Å.

SUMMARY

Alkali metal coatings exhibit properties which are useful in suppressing sputter-induced erosion and limiting plasma impurity influx from first wall and limiter surfaces. Since the secondary ion fraction is one of the key properties for this application, SIMS is virtually a mandatory experimental technique. Information on surface and near-surface composition and bond character are also desired. Of the conventional surface analysis techniques, this need is perhaps best met by a combination of AES, XPS and ISS. Useful information is also supplied by a variant of SIMS i.e. analysis of the secondary ion energy distribution. The ion beam based techniques alter the surface composition and depth profile of the alloys studied, but in so doing they simulate the fusion reactor environment. A systematic study must therefore be able to vary the beam parameters over a wide range and include sputtering by helium and hydrogen isotopes.

A single atomic layer of lithium can substantially reduce both the self-sputtering and the low energy light ion sputtering yield of the substrate material. The normal operating conditions of a plasma device provide an environment which promotes high lithium concentrations at the surface and near-surface regions of dilute lithium-bearing alloys. A systematic study is being undertaken to determine the extent to which alkali metal-bearing alloys can be used to improve the performance of magnetic confinement fusion devices.

REFERENCES

1. Alan R. Krauss and Dieter M. Gruen, J. Nucl. Mater. 103 & 104 (1981) 239.
2. A. Krauss and D. Gruen, J. Nucl. Mater. 85 & 86 (1979) 1179.
3. A. R. Krauss and D. M. Gruen, J. Nucl. Mater. 93 & 94 (1980) 686.
4. M. W. Thompson, Phil. Mag. 18 (1968) 377.
5. M. Bernheim, J. Rebière and G. Slodzian, in "Secondary Ion Mass Spectrometry (SIMS II)", ed. A. Benninghoven, C. A. Evans, Jr., R. A. Powell, R. Shimizu and H. A. Storms, Springer-Verlag, New York, 1979, 40.
6. I. Langmuir and K. H. Kingdon, Proc. Roy. Soc. (London), 107 (1925) 61.
7. I. Langmuir, J. Amer. Chem. Soc. 54 (1932) 61.
8. J. P. Blewett and E. J. Jones, Phys.Rev. 50 (1936) 465.
9. T. Okutani and R. Shimizu, Surface Sci. 88 (1979) L51.
10. A. R. Krauss, D. M. Gruen and A. B. DeWald, Proc. 9th Symp. Engineering Problems of Fusion Research, Oct. 26-29, 1981, Chicago, IL, USA.
11. A. B. DeWald, J. N. Davidson, A. R. Krauss and D. M. Gruen, Proc. Fifth Int. Conf. Plasma Surface Interactions in Controlled Fusion Devices, May 3-7, 1982, Gatlinburg, TN, USA.
12. F. Williams and D. Nason, Surf. Sci. 45 (1974) 377.
13. H. Wiedersich, to be published in "Surface Modification and Alloying," J. M. Poate and G. Foti, eds. NATO Materials Science Series, Plenum, NY.
14. L. E. Rehn, S. Danyluk and H. Wiedersich, Phys. Rev. Lett. 43 (1979) 1764.
15. R. F. Goff, J. Vac. Sci. Technol. 10 (1973) 355.
16. R. E. Honig and W. L. Harrington, Thin Solid Films 19 (1973) 43.
17. Handbook of X-ray Photoelectron Spectroscopy, G. E. Muilenburg ed. Perkin-Elmer, MN 1979.
18. Handbook of Auger Electron Spectroscopy, L. E. Davis, N. C. MacDonald, P. W. Palmberg, G. E. Riach and R. E. Weber, Physical Electronics Inc., MN 1976.
19. D. M. Gruen, A. R. Krauss, M. H. Mendelsohn and S. Susman, Proc. 5th Int'l. Conf. on Plasma Surface Interactions in Controlled Fusion Devices, May 3-7, 1982, Gatlinburg, TN.
20. A. Benninghoven, Surf. Sci. 35 (1973) 457.

FIGURE CAPTIONS

Figure 1. Probability that a secondary ion with kinetic energy E will undergo charge-exchange neutralization before it is returned to the emitting surface by the sheath potential V_s.

Figure 2. Plot of the secondary ion fraction for forty-two elements. Open symbols represent nominally clean surfaces and filled symbols are for oxygen-covered surfaces. (from ref. 2)

Figure 3. Experimental setup: CMA = cylindrical mirror analyzer, FC = Faraday cup, DIG = differential ion gun, ISS = ion scattering spectrometer, SIMS = secondary ion mass spectrometer.

Figure 4. XPS measurement of the potassium concentration during deposition and sputtering with a 1 keV He^+ beam, showing an abrupt change in the sputter-induced erosion rate. The two symbols (●) and (▲) correspond to separate runs with the sample at ground potential and biased -21 V.

Figure 5. Secondary ion yield versus fluence of the primary ion beam. The solid and dashed lines represent different fits to the data.

Figure 6. Kinetic energy distributions of secondary ions of three elemental metals, a potassium monolayer on a Mo substrate, and lithium in a Cu-Li alloy.

Figure 7. Results of TRIM calculation for the deuteron sputtering yield of copper from bulk copper, and copper and from a sample consisting of one monolayer of lithium on a copper substrate, with and without a hydrogen layer on the lithium.

Figure 8. First layer concentration for seven different alloys of Li in Al resulting from Gibbsian segregation. The bulk Li concentrations are: 10 PPM (▶), 50 PPM (●), 100 PPM (■), 500 PPM (◁), .005 (▷), .01 (○) and .05 (□).

Figure 9. Gibbsian segregation profile for an alloy consisting of 5% Li in Al at 773°K.

Figure 10. Lithium secondary ion yield during a heating sequence from room temperature to 300°C.

Figure 11. Lithium and aluminum secondary ion yield during a heating sequence from 300°C to 440°C.

Figure 12. Lithium secondary ion profile after quenching from 490°C.

Figure 1

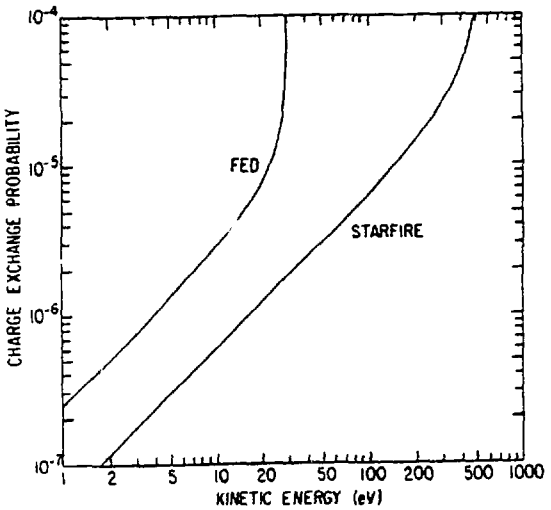

Figure 2

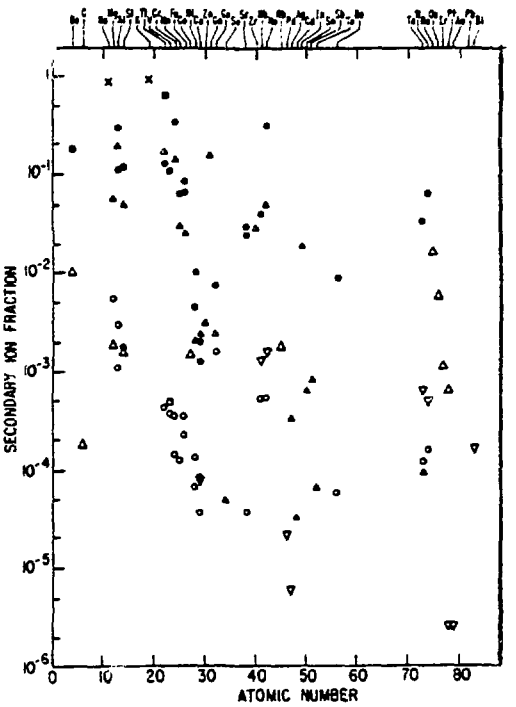

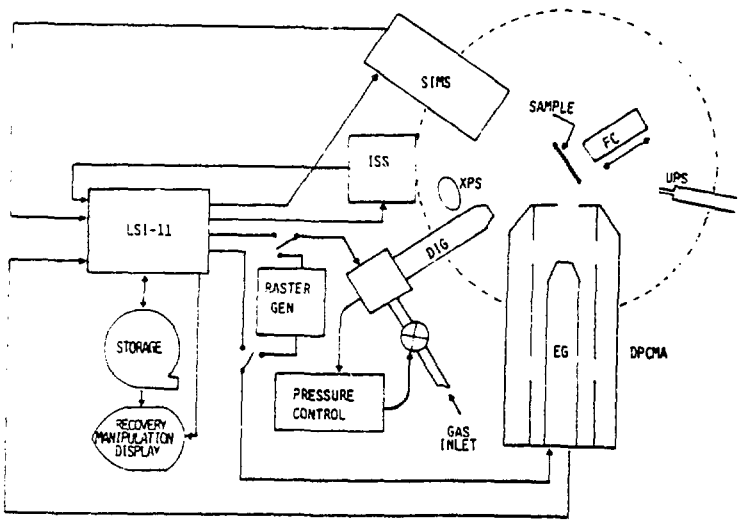

Figure 3

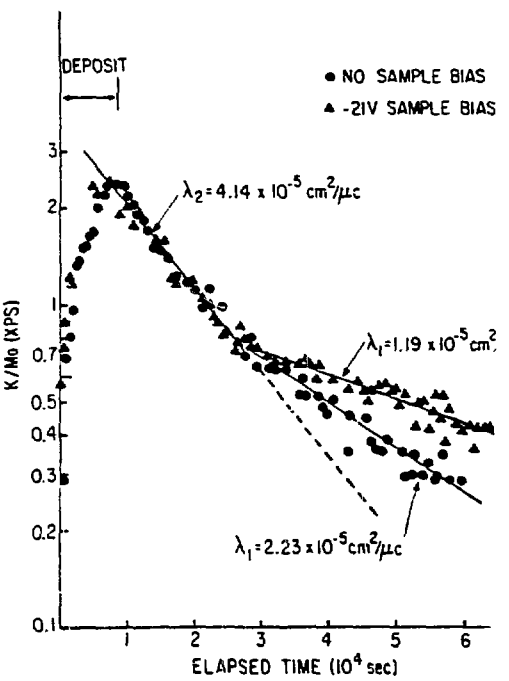

Figure 4

Figure 5

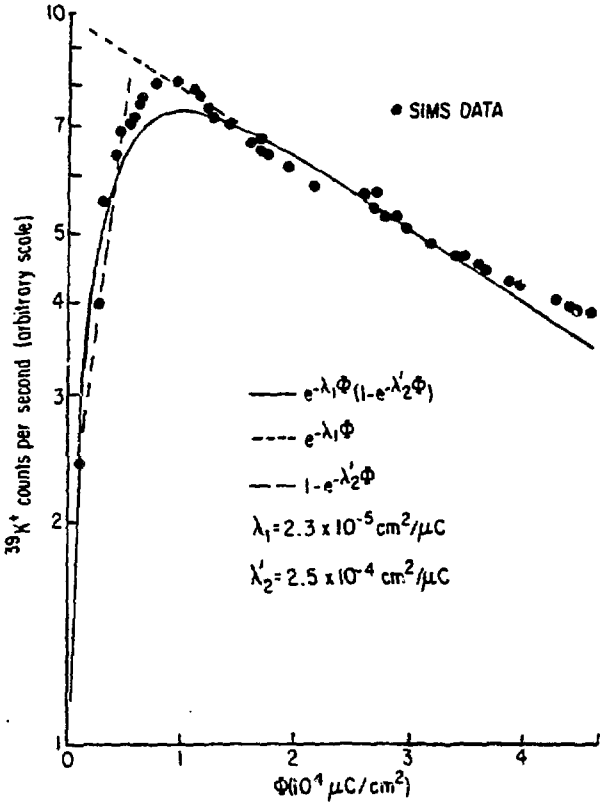

Figure 6

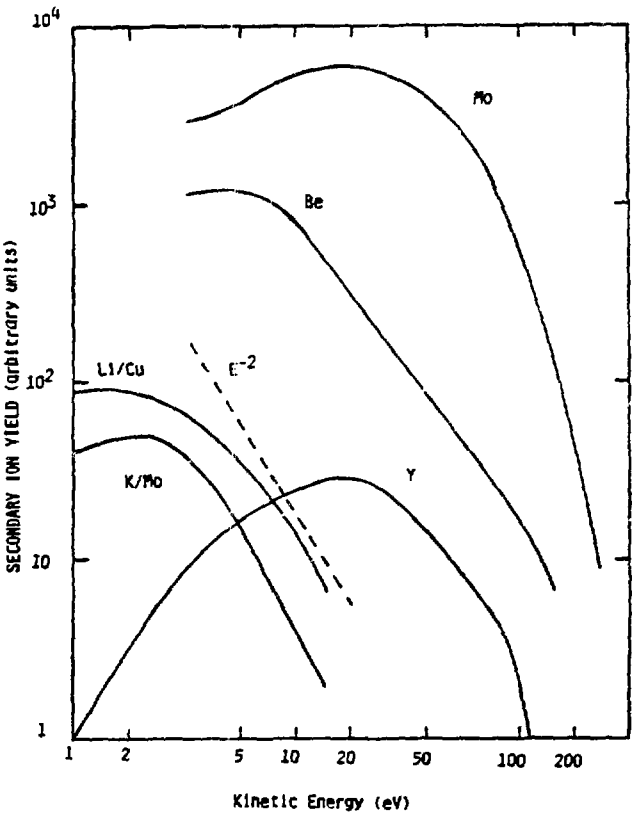

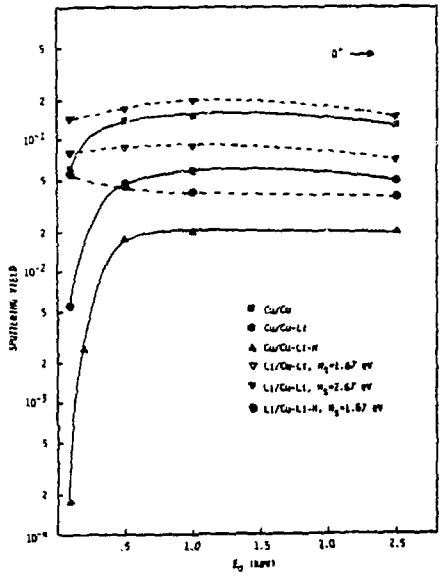

Figure 7

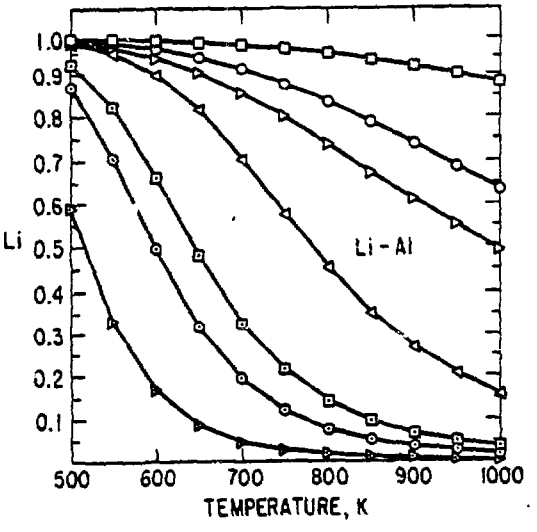

Figure 8

Figure 9

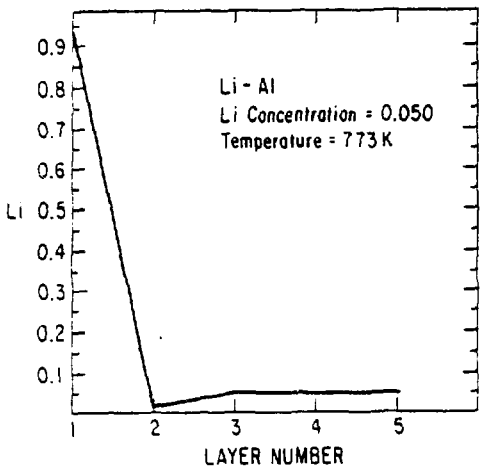

Figure 10

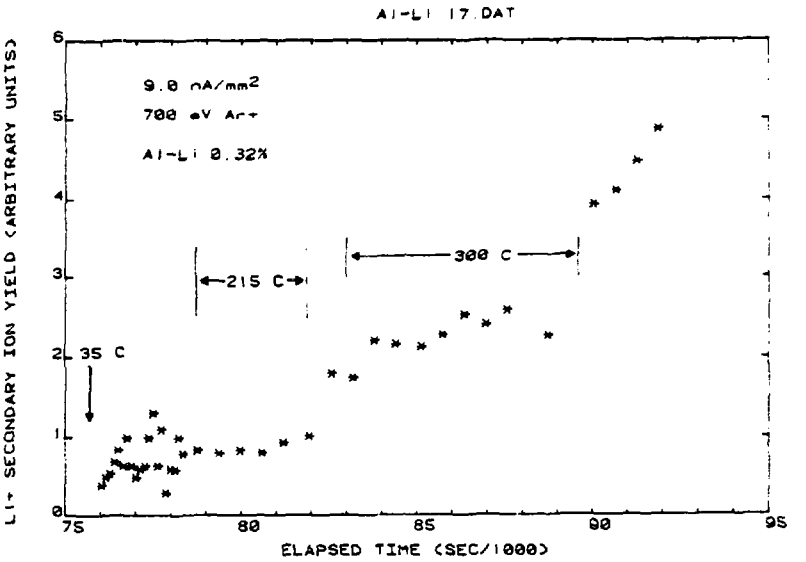

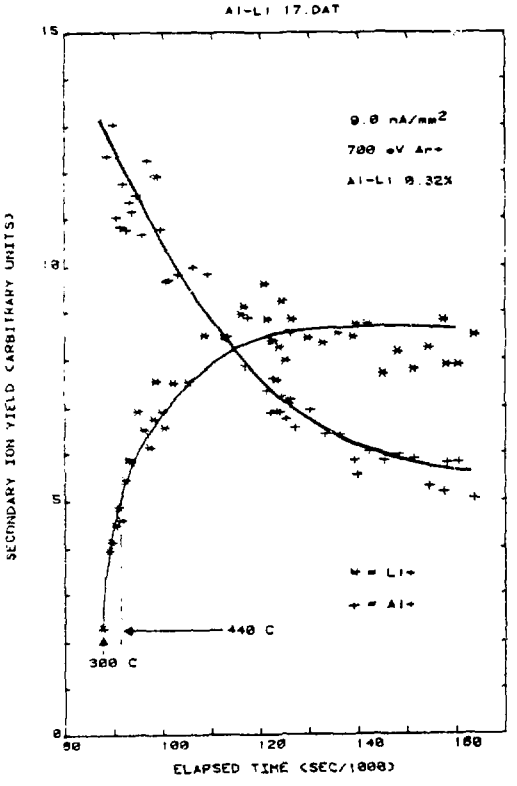

Figure 11

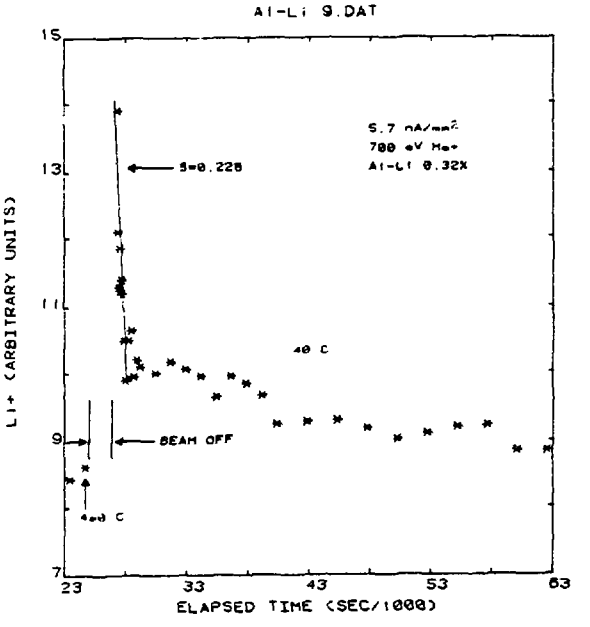

Figure 12